PNAS

Supporting Information for

Nanoparticle Elasticity Regulates the Formation of Cell Membrane Coated Nanoparticles and Their Nano-Bio Interactions

Da Zou [a, b], Zeming Wu [c], Xin Yi [c], Yue Hui [d], Guangze Yang [b, d], Yun Liu [b, d], Jisi Teng [b], Haofei Wang [b], Anastasia Brooks [a], Haolu Wang [a], Xin Liu [a], Zhi Ping Xu [b], Michael S. Roberts [a, e, f] *, Huajian Gao [g, h] *, Chun-Xia Zhao [b, d] *

a. Therapeutics Research Group, University of Queensland Diamantina Institute, The University of Queensland, Woolloongabba, QLD, Australia
b. Australian Institute for Bioengineering and Nanotechnology, The University of Queensland, St. Lucia, QLD, Australia
c. Department of Mechanics and Engineering Science, College of Engineering, Peking University, Beijing, China
d. School of Chemical Engineering and Advanced Materials, The University of Adelaide, Adelaide, SA, Australia
e. Clinical and Health Sciences, University of South Australia, Adelaide, SA, Australia
f. Therapeutics Research Centre, Basil Hetzel Institute for Translational Medical Research, The Queen Elizabeth Hospital, Woodville South, SA, Adelaide, Australia
g. School of Mechanical and Aerospace Engineering, Nanyang Technological University, Singapore, Singapore
h. Institute of High Performance Computing, A*STAR, Singapore, Singapore
*Corresponding author. Email: m.roberts@uq.edu.au (M. R.); huajian.gao@ntu.edu.sg (H.G.); chunxia.zhao@adelaide.edu.au (C.-X.Z.)

This PDF file includes:

Supporting Information Text

Theoretical calculation method

Mechanical properties of soft and hard nanocapsule shells

For a given indentation depth δ significant smaller than the capsule shell thickness h, computational studies indicate that the relationship between the load F and indentation depth δ can be well captured by the Reissner's formula on thin shell deformation as (1), (2)

$$F = \frac{4Eh^2\delta}{R\sqrt{3(1-\nu^2)}}, \tag{1}$$

where E and ν denote the Young's modulus and Poisson ratio of the capsule material (soft or hard SNs here), and R is the nanocapsule radius. Having knowledge of the force-indentation depth (F-δ) curves from experiments (**fig. S3**), values of the Young's modulus E of soft and hard nanocapsules are obtained as E_{TEVS} = 44 MPa and E_{TEOS} = 2.3 GPa, respectively, with h = 7 nm, ν = 0.5, R_{TEVS} = 86.3 nm, and R_{TEOS} = 112.45 nm.

Membrane wrapping of spherical polymer nanocapsules

The thin-shelled nanocapsule is assumed to undergo an axisymmetric deformation during the adhesive wrapping by the cell membrane (**Fig. 5A**). Before the wrapping process starts, the nanocapsule of an initial spherical shape with radius R is at a stress-free state. Characterizing the nanocapsule-membrane system in a cylindrical coordinate (r,ϕ,z), material point of the nanocapsule at ($r = r_0$, $z = z_0$) in the undeformed reference configuration can also be parameterized by coordinate (s_0,ψ_0) with geometrical relations $\mathrm{d}r_0/\mathrm{d}s_0 = \cos\psi_0$ and $\mathrm{d}z_0/\mathrm{d}s_0 = \sin\psi_0$, where s_0 is the arclength measured along the meridian of the capsule layer from the bottom pole in the reference configuration and $\psi_0 (= s_0/R)$ is the tangent angle.

As the membrane wraps around the nanocapsule, the nanocapsule material point (s_0,ψ_0) located at (r_0,z_0) is displaced by the cell membrane to (r,z) in the deformed configuration. Introducing the arclength s and tangent angle ψ of the deformed nanocapsule, (r,z) in the deformed configuration can be presented in a coordinate (s,ψ) with geometric relations $\mathrm{d}r/\mathrm{d}s = \cos\psi$ and $\mathrm{d}z/\mathrm{d}s = \sin\psi$. Then one has the longitudinal stretch $\lambda_s = \mathrm{d}s/\mathrm{d}s_0$ and latitudinal stretch $\lambda_\phi = r/r_0$ for the deformed nanocapsule in the meridional and circumferential directions, respectively.

The nanocapsule modeled as a linearly elastic isotropic thin shell has strain energy density W_{s} as (3)

$$W_{\mathrm{s}} = \frac{Eh}{2(1-\nu^2)}(e_s^2 + 2\nu e_s e_\phi + e_\phi^2) + \frac{B}{2}(C_s^2 + 2\nu C_s C_\phi + C_\phi^2), \tag{2}$$

where E is the Young's modulus, ν is the Poisson ratio, h is the shell thickness, and $e_s = \lambda_s - 1$ and $e_\phi = \lambda_\phi - 1$ are the meridional and circumferential strains, respectively; $B = Eh^3/[12(1-\nu^2)]$ is the bending rigidity of the thin shell, and $C_s = \lambda_s c_s - 1/a$ and $C_\phi = \lambda_\phi c_\phi - 1/a$ are the meridional and circumferential bending strains, respectively, with the meridional curvature $c_s = \mathrm{d}\psi/\mathrm{d}s$ and circumferential curvature $c_\phi = \sin\psi/r$.

The density of the elastic energy change of the cell membrane is (4)

$$W_{\mathrm{m}} = 2\kappa H^2 + \sigma(1 - \cos\psi_{\mathrm{m}}), \tag{3}$$

where κ, $H = (\mathrm{d}\psi_{\mathrm{m}}/\mathrm{d}t + \sin\psi_{\mathrm{m}}/r)/2$, ψ_{m}, and s_{m} are the bending stiffness, mean curvature, tangent angle, and arclength of the cell membrane, respectively. A representative value of κ is 20 $k_{\mathrm{B}}T$. Having Eqs. (2) and (3), the total system energy E_{tot} is

$$E_{\mathrm{tot}} = \int_0^{\pi R} 2\pi r_0 W_{\mathrm{s}} \mathrm{d}s_0 + \int_0^{\infty} 2\pi r W_{\mathrm{m}} \mathrm{d}s_{\mathrm{m}} - \gamma A_{\mathrm{c}}, \tag{4}$$

where γ is the adhesion energy and $A_{\mathrm{c}} = \int_0^a 2\pi r \mathrm{d}s$ is the contact area with a as the arclength at the contact edge. That contact edge in the reference configuration is located at $s_0 = a_0$. The wrapping degree f is defined as the contact area in the reference configuration divided by the total surface area of the undeformed nanocapsule, written as $f = \int_0^{a_0} 2\pi r_0 \mathrm{d}s_0 / (4\pi R^2)$.

To determine the minimum energy state at given f, the interior point optimization method is employed to minimize E_{tot}. The tangent angle ψ and longitudinal stretch λ_s in the inner free and adhesion regions as well as the tangent angle ψ_m in the outer free membrane are approximated by cubic B-spline functions (5). Each B-spline function is determined by a set of control points and their corresponding cubic basis functions. Then E_{tot} as a combination of $\psi(s_0)$, $\lambda_s(s_0)$ and $\psi_m(s_m)$ at given f and γ can be represented as a function of all control points, whose values are determined via energy minimization. During the nonlinear minimization, boundary and constraint conditions below provide input parameters or act as equality constraints. At $s_m \to \infty$, the outer free membrane is flat with $\psi_m = 0$. At the south and north poles of the nanocapsule, $\psi(s_0 = 0) = 0$ and $\psi(s_0 = \pi R) = \pi$. At the contact edge, the continuity of tangent angles and (r,z) coordinate are required. Once ψ, ψ_m, and λ_s are known, the total system energy and corresponding shapes of the nanocapsule and cell membrane can be determined.

Fig. 5B left shows the profile of elastic energy E_{el} ($= E_{tot} + \gamma A_c$) for hard and soft nanocapsule at $\sigma R^2/\kappa = 5$ and $\gamma = 0$. Here only the cases of vanishing γ are presented. Further numerical results indicate that $\gamma R^2/\kappa$ of practical interest has negligible influence on the elastic energy profiles and system configurations as the nanocapsule shell of high resistance to stretching exhibits slight area dilatation. **Fig. 5B** right shows selected wrapping configurations for rigid and soft nanocapsules. **Fig. 5** demonstrate that soft and rigid nanocapsules show infinitesimal difference in the wrapping energy and configurations, indicating that the mechanical behaviors of wrapping around spherical soft and hard nanocapsules can be modeled as the wrapping around spherical rigid nanoparticles.

Kinetics of receptor-mediated wrapping of rigid spherical nanoparticles

To investigate the kinetics of receptor-mediated wrapping of spherical rigid nanoparticles, here we consider an initially flat cell membrane patch containing diffusive receptors wrapping around a spherical rigid nanocapsule coated with uniformly distributed immobile ligands of density ξ_L. Before the nanocapsule contacts the cell membrane, the receptors are assumed to be uniformly distributed with a density of $\xi_0 (< \xi_L)$. Upon contact, each ligand within the contact region binds specifically with a receptor, and the density of receptors therein is raised from ξ_0 to ξ_L (**Fig. 5C**). The system free energy is reduced by the receptor-ligand binding, which benefits the membrane wrapping around the nanocapsule at the cost of membrane deformation energy and reduced configurational entropy due to receptor immobilization. Accompanying the expansion of the contact region, receptors in the vicinity of the contact region are drawn toward the contact edge via diffusion, and a local depletion of receptors near the contact edge is formed. Consequently, a global receptor diffusion in the outer free membrane region to the binding site is induced. As long as the free energy reduction owing to receptor-ligand binding can compensate the energy cost mentioned above, the wrapping process continues. Counting from the moment of contact ($t = 0$), the nanocapsule is fully wrapped at time $t = t_w$ with t_w as the particle wrapping time. Eventually, the internalized nanoparticle pinches off from the cell membrane.

The wrapping process above can be described with a mechanical model taking into account both the cell membrane deformation and the evolution of receptor density $\xi(s_m,t)$ as a function of the membrane arclength s_m and time t, as proposed in refs (6), (7), and confirmed by molecular dynamics simulations (8). The evolution of receptor density $\xi(s_m,t)$ is characterized by the kinetics of receptor diffusion. Denoting the arclength of the contact region as $a(t)$, one has $a(0) = 0$ and $\xi(s_m,0) = \xi_0$ at $t = 0$. Receptor conservation requires $\partial[\int \xi_L dA_c + \int \xi(s_m,t) dA_{outer}]/\partial t = 0$, where A_c is the contact area and A_{outer} is the outer free membrane area. The diffusive flux of receptors, $j = j(s_m,t)$, is assumed to obey Fick's first law as (9)

$$j = -D\partial\xi/\partial s_m, \tag{5}$$

where D is the diffusivity of receptors in the outer free membrane. Substituting the continuity equation (9)

$$\partial\xi/\partial t = -r^{-1}\partial(rj)/\partial s_m \tag{6}$$

into the conservation equation yields

$$(2R^2/r_+)(\xi_L - \xi_+)\mathrm{d}f/\mathrm{d}t + j_+ = 0 \quad \text{or} \quad (\xi_L - \xi_+)\mathrm{d}a/\mathrm{d}t + j_+ = 0, \tag{7}$$

where $r_+(t) \equiv r(a_+,t)$, $j_+(t) \equiv j(a_+,t)$, and $\xi_+(t) \equiv \xi(a_+,t)$ represent corresponding values directly in front of the contact edge. In the derivation of Eq. (6), conditions of fixed total area of the cell membrane and $j = 0$ at the remote boundary have been used.

Substituting Eq. (5) into Eq. (6) yields the governing equation for the receptor density evolution in the outer free membrane as

$$\frac{\partial \xi(s_{\rm m},t)}{\partial t} = D\left(\frac{\partial^2 \xi}{\partial s_{\rm m}^2} + \frac{\cos\psi_{\rm m}}{r}\frac{\partial \xi}{\partial s_{\rm m}}\right), \quad s_{\rm m} > a(t). \tag{8}$$

The profiles of r and $\psi_{\rm m}$ are given by the equilibrium solutions obtained from the energy minimization in the previous section.

To obtain the nanoparticle wrapping time $t_{\rm w} = \int_0^1 ({\rm d}f/{\rm d}t)^{-1}{\rm d}f$, one needs to evaluate the wrapping rate df/dt as a function of r_+, ξ_+ and j_+ (or equivalently $\partial\xi/\partial s_{\rm m}$ at $s_{\rm m} = a_+$) based on Eq. (7), and the procedure is as follows.

The total free energy $F(t)$ of the system consists of the energy of receptor-ligand binding, configurational entropy of receptors, and cell membrane deformation energy $E_{\rm el}$, and can be written as

$$F(t) = \int \xi_{\rm L} k_{\rm B}T\left(-e_{\rm RL} + \ln\frac{\xi_{\rm L}}{\xi_0}\right){\rm d}A_{\rm c} + \int \xi k_{\rm B}T\ln\frac{\xi}{\xi_0}{\rm d}A_{\rm outer} + E_{\rm el}, \tag{9}$$

where $k_{\rm B}T = 4.1\times10^{-21}$ J and $k_{\rm B}Te_{\rm RL}$ denotes the binding energy per receptor-ligand bond of around 10 $k_{\rm B}T$ to 25 $k_{\rm B}T$ [Leck01]; $k_{\rm B}T\ln(\xi_{\rm L}/\xi_0)$ and $k_{\rm B}T\ln(\xi/\xi_0)$ are the free energy per receptor associated with the relative entropy of the bound and free receptors, respectively. Differentiation of $F(t)$ in Eq. (9) with respect to time t leads to

$$\frac{{\rm d}F(t)}{{\rm d}t} = -\left[4\pi R^2 k_{\rm B}T\left(e_{\rm RL}\xi_{\rm L} - \xi_{\rm L}\ln\frac{\xi_{\rm L}}{\xi_+} + \xi_{\rm L} - \xi_+\right) - \frac{{\rm d}E_{\rm el}}{{\rm d}f}\right]\frac{{\rm d}f(t)}{{\rm d}t} - \int Dk_{\rm B}T\xi\left(\frac{\partial\chi}{\partial s_{\rm m}}\right)^2{\rm d}A_{\rm outer}, \tag{10}$$

where $\chi(s,t) = \ln(\xi/\xi_0) + 1$ is the local chemical potential per receptor. Balancing the rate of free energy reduction in the wrapping process with the rate of energy dissipation associated with receptor transport, the first term in the above equation must vanish (6). Therefore, one has

$$k_{\rm B}T\xi_{\rm L}\left(e_{\rm RL} + \ln\frac{\xi_+}{\xi_{\rm L}} + 1 - \frac{\xi_+}{\xi_{\rm L}}\right) - \frac{1}{4\pi R^2}\frac{{\rm d}E_{\rm el}}{{\rm d}f} = 0, \tag{11}$$

which allows $\xi_+(t)$ to be determined at given a.

Once the receptor density profile $\xi(s_{\rm m},t_0)$ at $t = t_0$ during the initial stage of contact is known, one can determine $\xi(s_{\rm m},t)$ at $t > t_0$ by solving Eq. (8) via the finite difference method, using $\xi_+(t)$ to determine $j_+(t)$ in Eq. (5), and then obtaining df/dt with knowledge of $\xi_+(t)$, $j_+(t)$ and $r_+(t)$ from Eq. (7).

The procedure for obtaining $\xi(s_{\rm m},t_0)$ is as follows. At the initial stage of contact, the contact size is much smaller than the membrane size and the outer free membrane is almost flat. Therefore, the membrane at the moment $t = t_0$ can be regarded approximately as a flat membrane of an infinite size and Eq. (8) becomes $\partial\xi/\partial t = D\partial^2\xi/\partial s_{\rm m}^2$ over $a(t_0) < s < \infty$, which can be solved analytically as (6)

$$\xi(s_{\rm m},t_0) = \xi_0 + \Lambda E_1(s_{\rm m}^2/(4Dt_0)), \tag{12}$$

where $E_1(x) = \int_1^\infty u^{-1}e^{-ux}{\rm d}u$ is the exponential integral and Λ is a constant of integration. This solution satisfies the diffusion equation and boundary condition $\xi(s_{\rm m},0) = \xi_0$ and $\xi(s_{\rm m},t_0)\to\xi_0$, $j(s_{\rm m},t_0)\to0$ as $s_{\rm m}\to\infty$. Substituting Eq. (11) into Eq. (7) gives $\Lambda = -\alpha^2\exp(\alpha^2)(\xi_{\rm L} - \xi_0)/(1 - g)$ with $g = \alpha^2\exp(\alpha^2)E_1(\alpha^2)$ and α as a constant to be determined. Then one has $\xi_+/\xi_{\rm L} = (\xi_0/\xi_{\rm L} - g)/(1 - g)$. Substituting Eq. (12) and $\xi_+/\xi_{\rm L}$ into Eq. (11), α can be determined. Once α is known, $\xi(s_{\rm m},t_0)$ at the initial stage of contact is fully given by Eq. (12). With the knowledge of $\xi(s_{\rm m},t_0)$, $\xi_+(t)$, profiles of $E_{\rm el}(f)$ or d$E_{\rm el}$/df (Fig. 4a), and diffusion equation (8), the wrapping rate df/dt can be determined through Eq. (7). Then the nanoparticle wrapping time $t_{\rm w}$ is obtained as $t_{\rm w} = \int_0^1 ({\rm d}f/{\rm d}t)^{-1}{\rm d}f$.

Figures

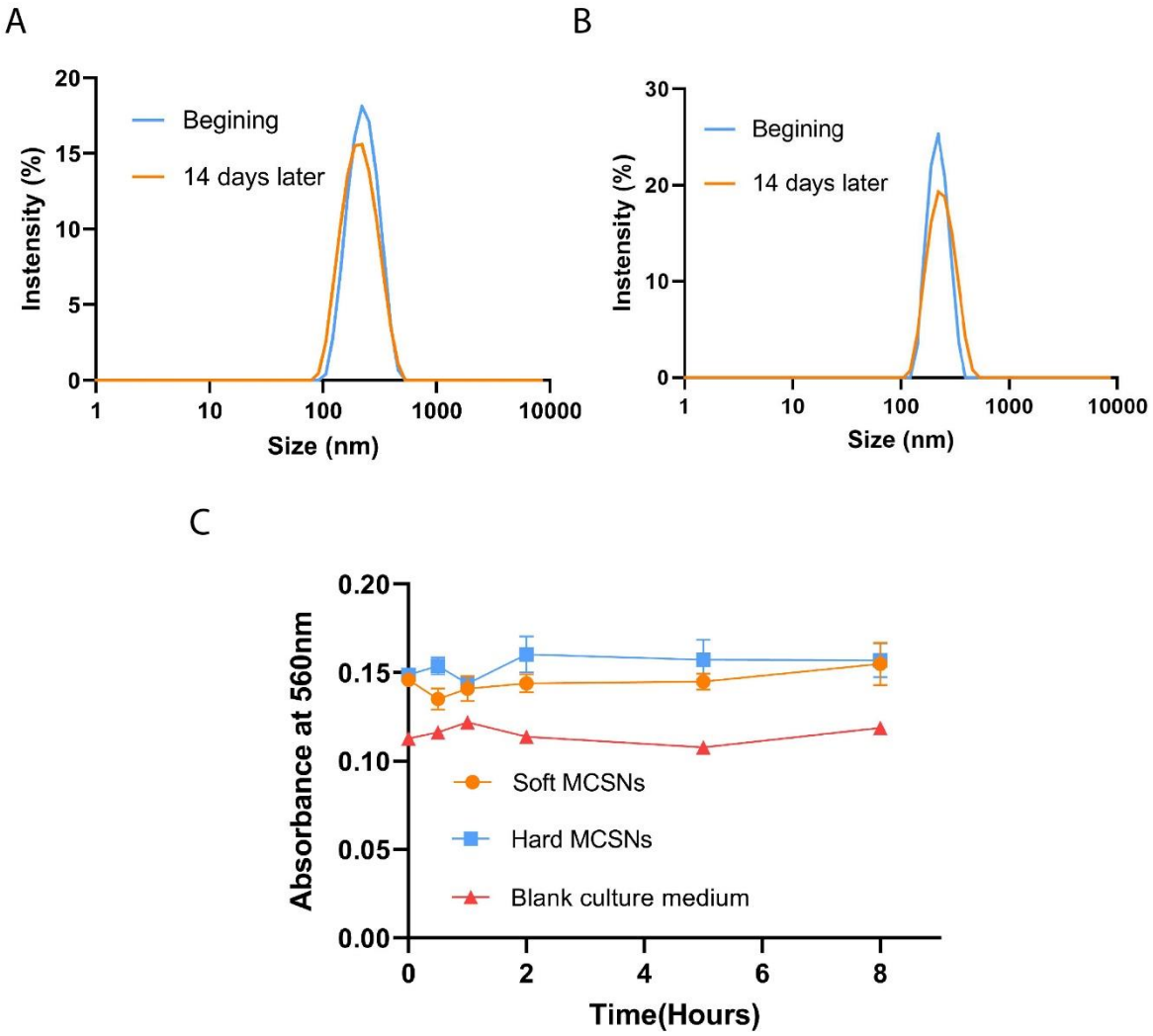

Fig. S1 Stability of MCSNs. (**A**) Stability of soft MCSNs in PBS buffer, as measured by DLS. (**B**) Stability of hard MCSNs in PBS buffer, as measured by DLS. (**C**) Stability of MCSNs in DMEM with 10% FBS, as measured by UV-vis, the values are means ± SD (n = 3).

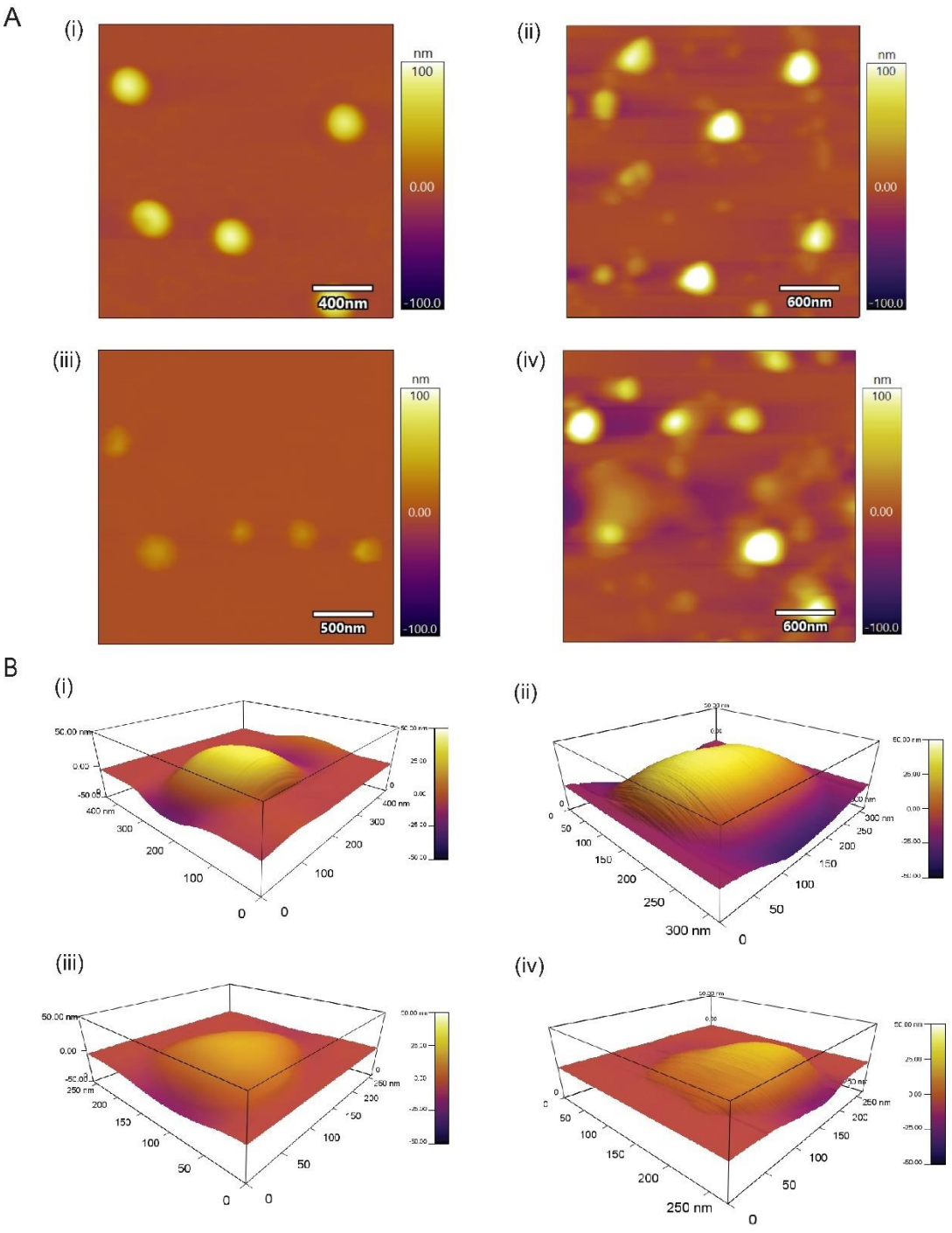
A
(i)
nm
100
0.00
-100.0
400nm
(ii)
nm
100
0.00
-100.0
600nm
(iii)
nm
100
0.00
-100.0
500nm
(iv)
nm
100
0.00
-100.0
600nm
B
(i)
(ii)
(iii)
(iv)
C
N.S.
2500
2000
1500
100
50
0
Young's modulus (MPa)
N.S.
PEG
MCSNs
Soft
Hard

Fig. S2 Mechanical properties of SNs and MCSNs. (**A**) AFM height profiles of **(i)** PEGylated hard SNs, **(ii)** hard MCSNs, **(iii)** PEGylated soft SNs, **(iv)** soft MCSNs. (**B**) Reconstructed 3D morphologies of **(i)** PEGylated hard SNs, **(ii)** hard MCSNs **(iii)** PEGylated soft SNs, **(iv)** soft MCSNs. (**C**) Young's moduli of soft and hard PEGylated SNs (PEG) and MCSNs, the values are means ± SD (n = 10).

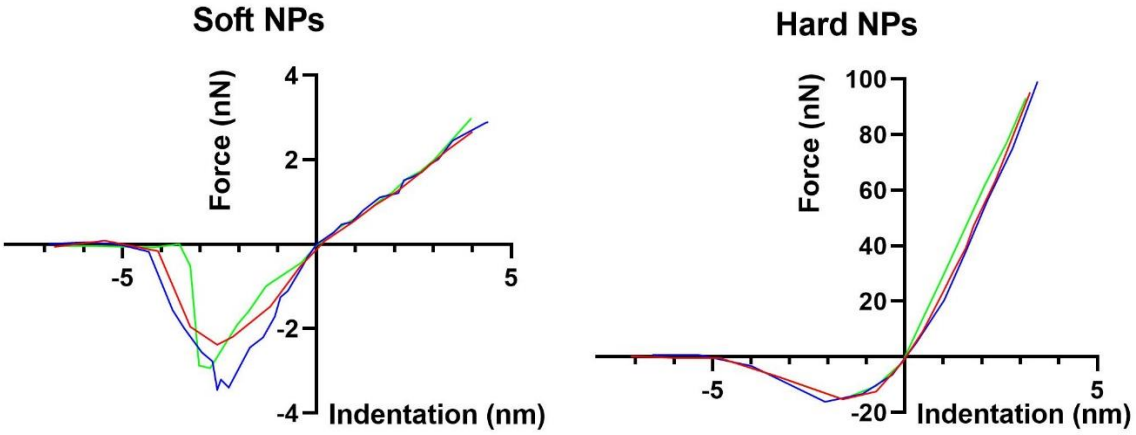

Fig. S3. Representative force-indentation curves. Representative force-indentation curves of soft (left) and hard (right) MCSNs. Calculated Young's modules were 44 ± 2.8 MPa (left) and 2.3 ± 0.1 GPa (right).

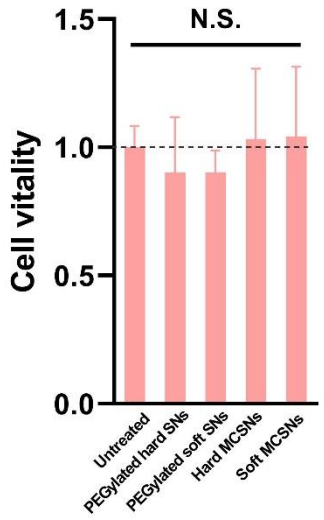

Fig. S4. Cell vitality tested by WST-1. Cell vitality of IHH cells under various treatments. The values are means ± SD (n = 8).

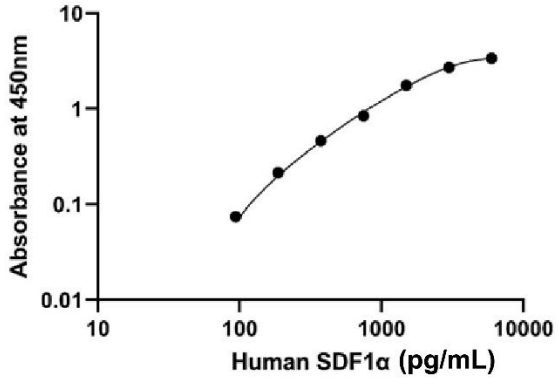

Fig. S5. Standard curve of SDF-1α for ELISA measurement.

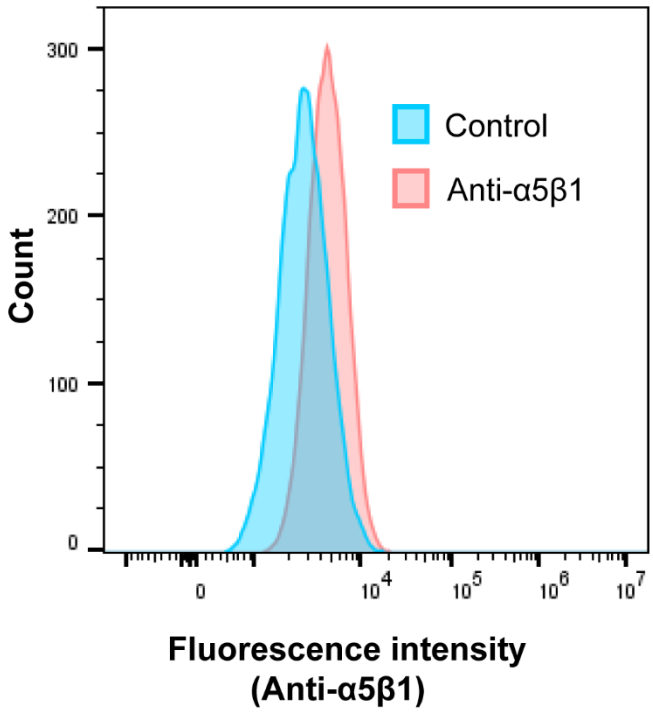

Fig. S6. Flow cytometry analysis of the presence of integrin α5β1. Flow cytometry analysis of the presence of integrin α5β1on the surface of IHH cells expressed by overlay distribution. Cell incubated with only secondary antibody was the control group.

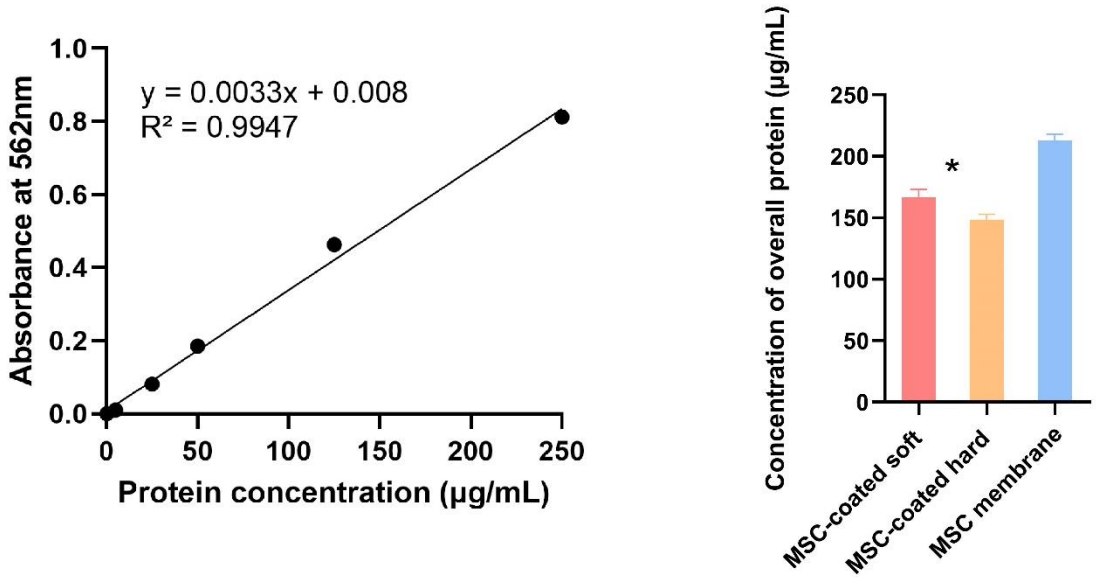

Fig. S7. BCA assay of overall protein concentration. Left**:** BCA assay standard curve calculated by the standard BSA solution. Right**:** BCA assay of overall protein concentration of soft and hard MCSNs. All values are means ± SD (n = 3, with *P < 0.05).

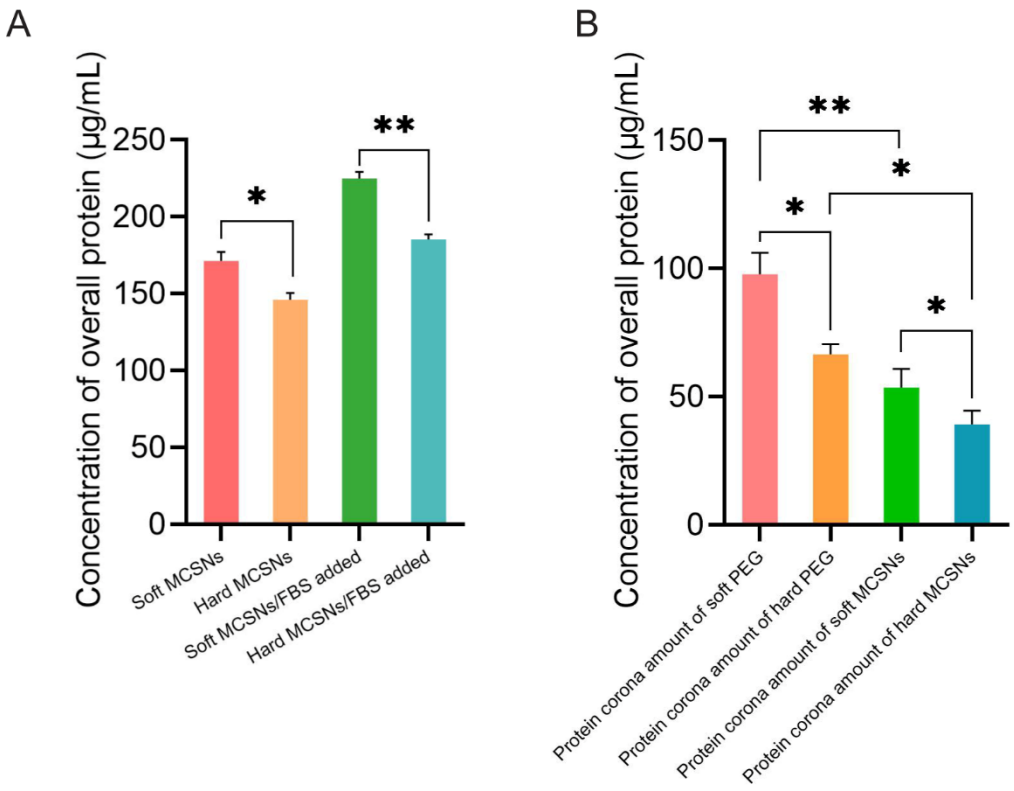

Fig. S8. Protein concentration measured using BCA assay. (A) Protein concentration of MCSNs with or without protein corona effect. **(B)** Concentration of protein corona on PEGylated nanoparticles and MCSNs. All values are means ± SD (n = 3, with *P < 0.05 and **P < 0.01).

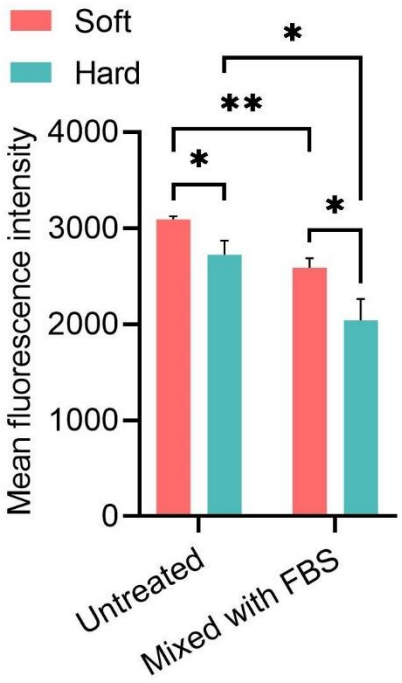

Fig. S9. Flow cytometry analysis of the presence of CXCR4 on the surface of soft and hard MCSNs with FBS treated for 4 hours. All values are means ± SD (n = 3, with *P < 0.05 and **P < 0.01).

A

Hard MCSNs	Long axis (nm)	Short axis (nm)	Dimension ratio		Soft MCSNs	Long axis (nm)	Short axis (nm)	Dimension ratio
	158.11	156.45	1.010			165.36	157.46	1.050
	107.7	103.09	1.044			171.54	149.67	1.146
	185.69	178.35	1.041			146.34	136.67	1.071
	196.16	159.99	1.226			181.07	171.29	1.057
	207.46	162.87	1.274			113.86	97.30	1.170
	210.29	198.46	1.060			217.62	184.56	1.179
	201.91	188.11	1.073			162.62	138.76	1.172
	125.00	119.16	1.049			145.22	119.71	1.213
	158.38	143.92	1.100			138.45	133.33	1.038
	109.61	105.40	1.010			126.14	115.24	1.095
Ave. ± S.D.	166.03 ± 38.27	151.58 ± 31.72	1.092 ± 0.082		Ave. ± S.D.	156.82 ± 28.24	140.40 ± 25.03	1.119 ± 0.060

B

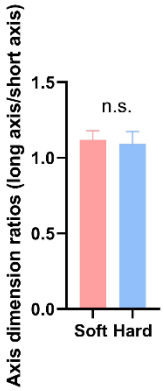

Fig. S10. Axis dimension ratio of the soft and hard MCSNs on cell surfaces. (**A**) value of axis. (**B**) Average of axis dimension ratios, measured by NanoMeasurer software (v. 1.2.5).

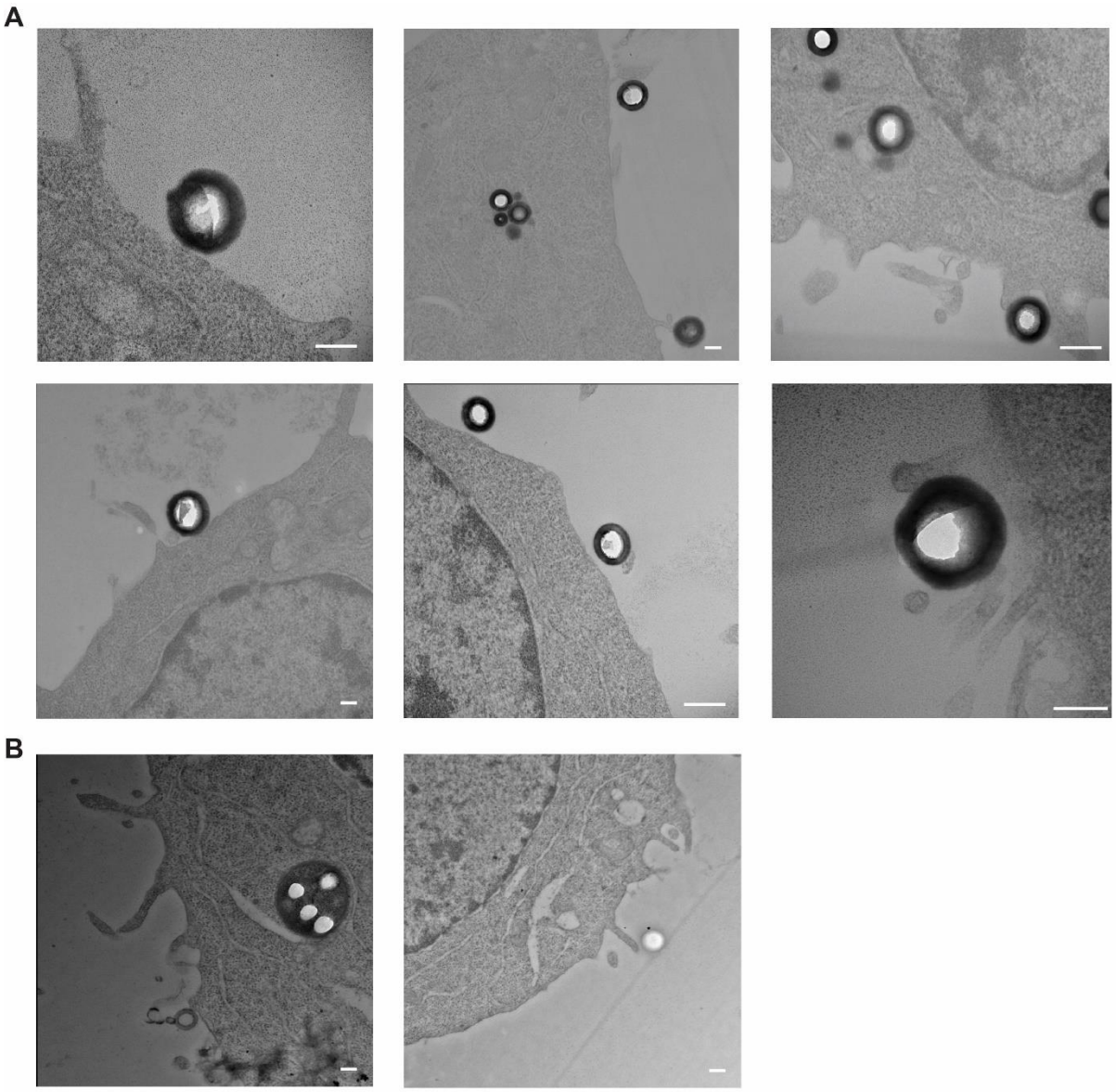

Fig. S11. TEM images of MCSNs co-incubated with macrophage cells. (**A**) TEM images of hard MCSNs co-incubated with macrophage cells. (**B**) TEM images of soft MCSNs co-incubated with macrophage cells.

Table S1. Parameters used in the theoretical model

Parameter	Significance
κ	Cell membrane bending rigidity
σ	Membrane tension
γ	Membrane-nanocapsule adhesion energy
R	Nanocapsule radius
B	Bending rigidity of the capsule thin shell
D	Diffusivity of ligands on cell membrane
ξ_0	Initial receptor density
ξ_L	Ligand density

SI References

1. J. D. Berry, S. Mettu, R. R. Dagastine, Precise measurements of capsule mechanical properties using indentation. *Soft Matter* **13**, 1943-1947 (2017).
2. E. Reissner, Stresses and Small Displacements of Shallow Spherical Shells. I. *Journal of Mathematics and Physics* **25**, 80-85 (1946).
3. S. Knoche, J. Kierfeld, Buckling of spherical capsules. *Phys. Rev. E Stat. Nonlin. Soft Matter Phys.* **84**, 046608 (2011).
4. W. Helfrich, Elastic properties of lipid bilayers: theory and possible experiments. *Z. Naturforsch. C* **28**, 693-703 (1973).
5. X. Yi, H. Gao, Cell membrane wrapping of a spherical thin elastic shell. *Soft Matter* **11**, 1107-1115 (2015).
6. H. Gao, W. Shi, L. B. Freund, Mechanics of receptor-mediated endocytosis. *Proc. Natl. Acad. Sci. U. S. A.* **102**, 9469 (2005).
7. X. Yi, H. Gao, Kinetics of receptor-mediated endocytosis of elastic nanoparticles. *Nanoscale* **9**, 454-463 (2017).
8. Z. Shen, H. Ye, X. Yi, Y. Li, Membrane Wrapping Efficiency of Elastic Nanoparticles during Endocytosis: Size and Shape Matter. *ACS Nano* **13**, 215-228 (2019).
9. J. Faraudo, Diffusion equation on curved surfaces. I. Theory and application to biological membranes. *The Journal of Chemical Physics* **116**, 5831-5841 (2002).